J. Membrane Biol. 37, 45–61 (1977)

Quantitative Electron Microscopical Studies on *in Vitro* Incubated Rabbit Gallbladder Epithelium

H. Blom and H.F. Helander

Department of Anatomy, University of Umeå, S-901 87 Umeå, Sweden

Received 25 January 1977; revised 6 April 1977

Summary. Pieces of rabbit gallbladders were incubated in vitro for 1 hr in Ringer's solution at 37° ("transporting epithelium"), or in Ringer's containing 1 mM ouabain ("inhibited epithelium"). The tissues were fixed in 2% glutaraldehyde, postfixed in OsO_4 and embedded in Epon. Stereological analysis was carried out on electron micrographs; with this type of analysis it is possible to obtain quantitative data for the three-dimensional structure of the tissue. The following data were obtained for crest transporting epithelium (crypt epithelium in parentheses): Epithelial height, 28 (18) μm; nucleus, 16.9 (18.7) % of cell volume; mitochondria, 18.7 (14.1) % of cytoplasmic volume; paracellular channels, 28.3 (11.0) % of epithelial volume; lateral plasma membrane, 4.1 (2.9) m^2/cm^3, and apical membrane, 0.5 (0.6) m^2/cm^3 of cell volume. The paracellular channels appeared as interconnected tissue sheets of a highly varying width. They were broader in the basal portion of the epithelium than in the apical portion; however, immediately above the basement membrane the channels became very narrow. The arithmetic mean width of the channels was 0.9 (0.2) μm and their length was in the range of 40–120 μm. Our stereological data seem compatible with the standing gradient model for water transport.

The ouabain inhibited cells were swollen with collapsed paracellular channels. It cannot be ruled out that volume changes occurred in the cells and the paracellular channels during the processing of the tissue. However, qualitatively the same morphology was observed by light microscopy of transporting and inhibited gallbladder epithelium fixed by freeze-drying and embedded in Epon. This constitutes a strong indication of the presence of such channels in the living, in vitro transporting rabbit gallbladder epithelium.

The gallbladder has been extensively used in studies of water and electrolyte transport, and on the basis of such studies theories have been advanced which have explained transport processes across simple epithelia. Diamond and Bossert (1967) focused attention on electrolyte pumps which, by osmotic forces, drag water into paracellular channels. The capacities of the transepithelial transport rest partly on the structural characteristics of the paracellular channels – length, width, and surface area are included among the parameters discussed (Diamond & Bossert,

1967; Smulders, Tormey & Wright, 1972; Hill, 1975). Yet stereological data on the ultrastructure of the gallbladder epithelium – as well as other fluid-transporting epithelia – are virtually nonexistent. Most quantitative morphological information from fluid-transporting epithelia is not based on a statistically correct sampling method, but certain micrographs have simply been considered "typical" and measurements from these have been reported. Yet there is such great variation in dimensions of epithelial structures within a section and between sections and preparations that no morphological measurements that dispense with statistical sampling can be taken seriously.

It is not just that statistical sampling is necessary. A further problem is that, even if there were absolutely no variability, measurements of a two-dimensional section would not correctly reveal the measurements of a three-dimensional structure. Consider, for example, a uniform population of spheres. If one sections the spheres at random and measures the diameters of the resulting circles, the measured diameters will range from zero to the actual diameter of the sphere, depending upon how far from the center of the sphere the plane of the section passed. Thus, naive measurement would yield a spuriously low value for the sphere's diameter. Yet, it is a well-defined problem in mathematics to determine the distribution of diameters measured from random sections through a sphere and, hence, to calculate the true diameter of the original sphere from random sections. This example illustrates the purpose of stereological analysis: to apply sampling techniques and statistical techniques to determine the correct dimensions of a three-dimensional structure seen in two-dimensional sections. The methods of stereological analysis have been discussed and developed in detail by Weibel (1969, 1973). In recent years stereological analysis has been used increasingly frequently in ultrastructural studies, but only sparsely in fluid transporting epithelia.

Stereological analysis is particulary important for fluid-transporting epithelia, since knowledge of the dimensions of the transporting channels is essential for evaluating theories of water transport (e.g., Diamond & Bossert, 1967; Hill, 1975). Despite the extensive literature measuring ultrastructural dimensions of epithelia and relating these dimensions to theories of transport, most of these measurements must be regarded with reserve because of the lack of any statistical sampling.

In the present study stereological data are provided for in vitro transporting and ouabain inhibited rabbit gallbladder epithelia. The figures are discussed in the light of some theoretical considerations on electrolyte and water transport.

Materials and Methods

Seven male rabbits (2.5–3.5 kg) of a local strain were used for the investigation. The rabbits were killed by an injection of air intravenously, and the gallbladder was rapidly taken out and transferred to NaCl-HCO_3-Ringer's solution (temp 4 °C, pH 7.4) gassed by O_2/CO_2 (95:5%). The composition of this solution was the same as described by Tormey and Diamond (1967). The corpus region of the gallbladder was used and was divided into two pieces. These procedures took about three min. One of the pieces was then transferred to a fresh Ringer's solution. The other portion was put into a flask with the same solution which, in addition, contained 1 mM ouabain. Both preparations were incubated under continuous gassing (O_2/CO_2, 95:5%) for 1 hr at 37° and were then fixed for 3 hr in an solution of 2% glutaraldehyde in Ringer's (temp 4°, pH 7.4). After rinsing in Ringer's, postfixation was carried out for 2 hr in 1% OsO_4 dissolved in Ringer's (temp 4°, pH 7.4). Subsequently the tissue was dehydrated in rising concentrations of ethanol and embedded in Epon. Tissue blocks were sectioned at a feeding rate of 80 nm per cycle, roughly perpendicular to the surface of the epithelium. The sections were placed on copper grids (one-hole or 75–100 mesh), contrasted with uranyl acetate and lead hydroxyde, and studied in a Siemens 1A or a Philips EM 300 electron microscope at original magnifications of approximately 3000–13,000×. Calibration of the magnification was performed using a carbon grating with 54,864 lines per inch.

The mucosa of the gallbladder is thrown into small folds or rugae, with intervening crypts. Electron micrographs were taken of the epithelium directly exposed to the gallbladder lumen ("crest cells") and of epithelium in the bottom of the crypts ("crypt cells") (Fig. 1).

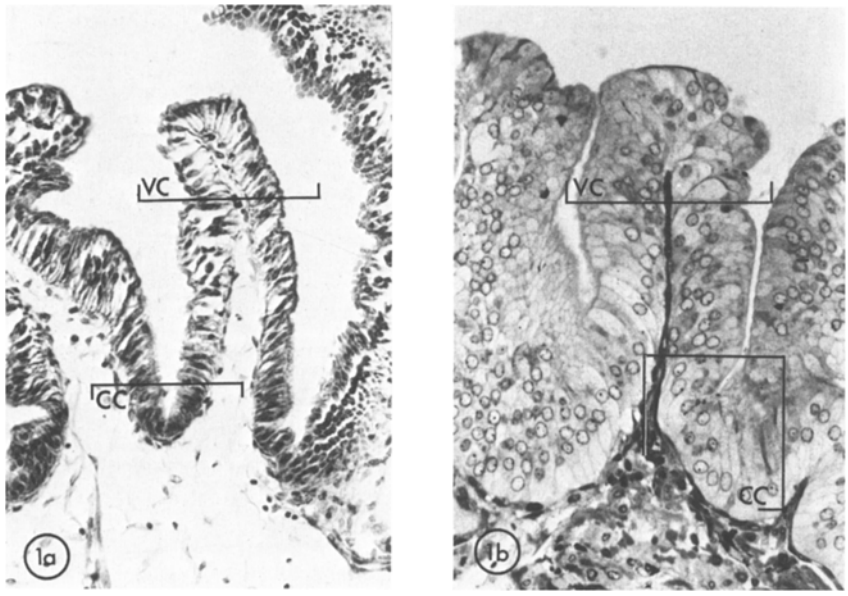

Fig. 1. Surveys of in vitro transporting (1*a*) and ouabain inhibited (1*b*) rabbit gallbladder epithelia. Paracellular channels are seen in the transporting, but not in the inhibited epithelium. *VC*: crest cells; *CC*: crypt cells. Formalin fixed paraffin sections. Hematoxyline eosin. 200×

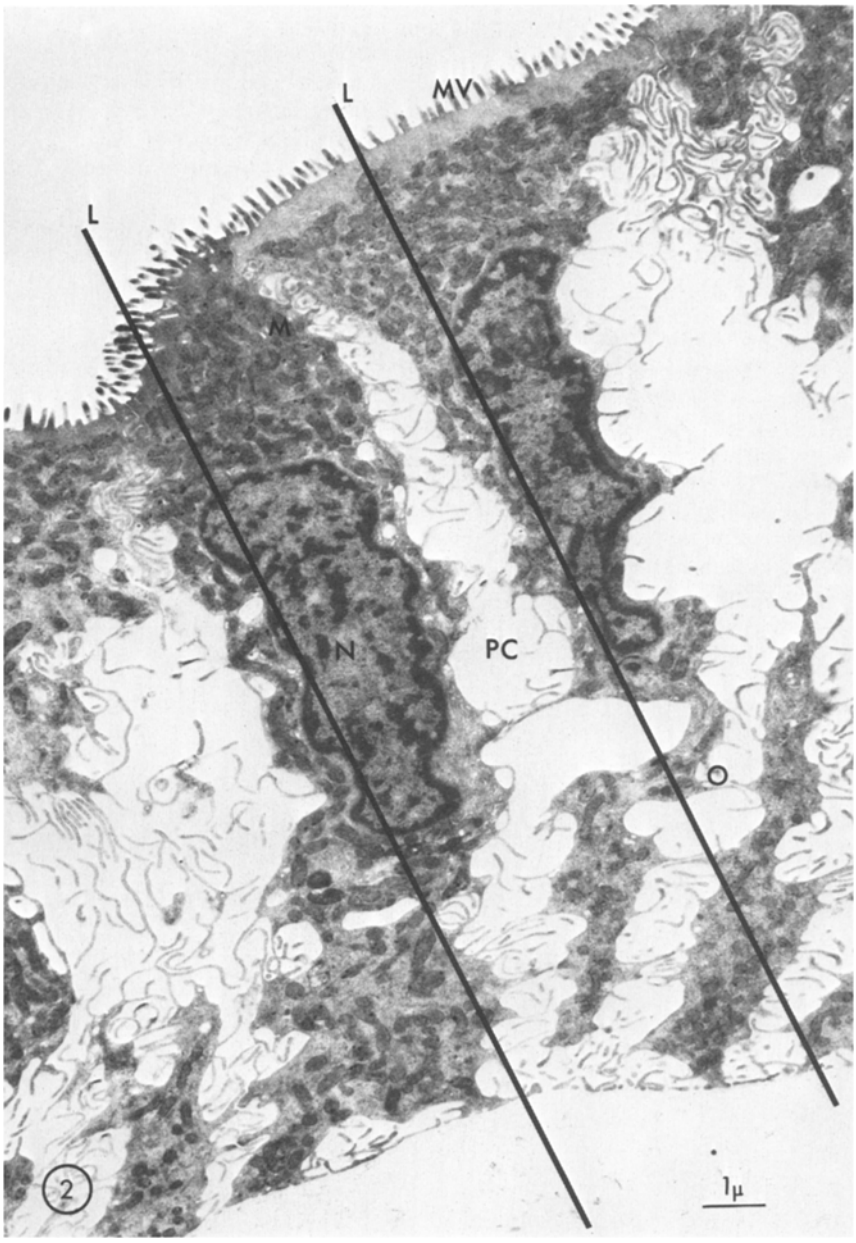

Fig. 2. Survey of transporting crest cells. Two parallel lines *L* limit the region in which the morphometric measurements were performed. The paracellular channels (*PC*) are irregularly formed, being narrow towards the surface of the epithelium and broader in the basal part. Numerous villi or ridges project into these channels, and sometimes such projections meet to produce a narrow orifice (*O*) in the channel. *N*: nucleus; *M*: mitochondria; *MV*: microvilli. 7600×

In each functional state (with and without ouabain) in each animal, 5 "regions" were selected randomly (partly according to the method described by Weibel, 1973) from the micrographs of the crest cells and 5 from the crypts cells. These regions were used for the measurements and were bordered by two parallel lines about 2–12 μm apart and by the apical and basal surfaces of the epithelial cells (Fig. 2). The regions were relatively narrow, so that in some micrographs they would mainly contain epithelial cells, in others mainly paracellular channels. However, since many regions were analyzed, the mean values were probably not affected.

The nuclear volume density V_{Vn} was calculated in reference to the total cell volume (including the nuclei), and the mitochondrial volume density (V_{Vm}) in reference to the cytoplasmic volume (excluding the nuclei). The paracellular channel volume density (V_{Vpc}) was calculated in reference to the total epithelial volume. These volume densities were determined using the point-counting method (Weibel, 1973). For this purpose a square lattice with the lines 0.5–0.8 μm apart was placed at random over each micrograph. The intersections of lines served as test points; the number of test points over each epithelial region was usually 120–300.

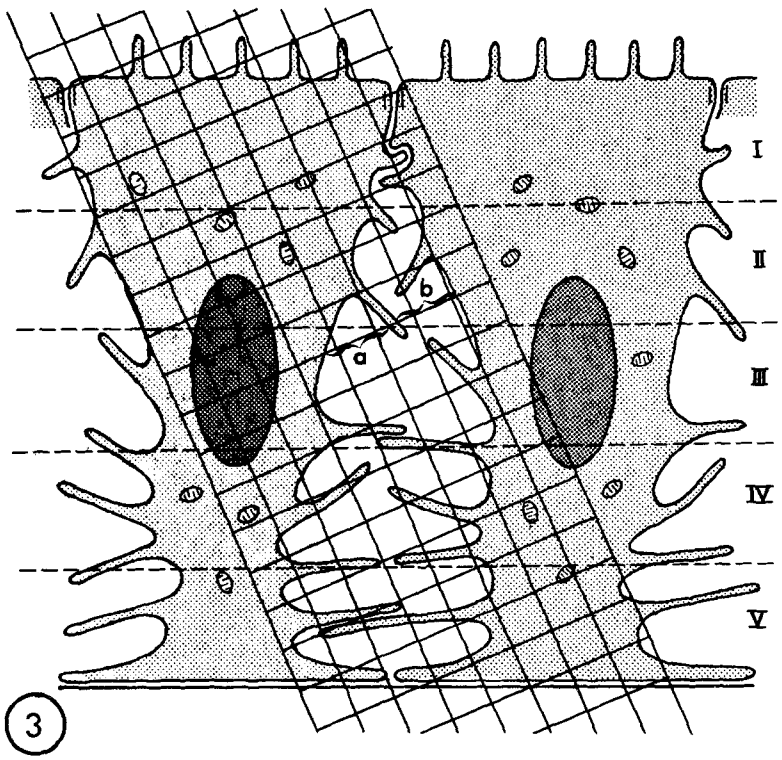

Fig. 3. Schematic representation of two gallbladder cells with an intervening paracellular channel. A grid, similar to that used for surface density determinations, is superimposed. This type of grid was also employed for measuring the width of the paracellular channels. For this purpose, the length of the test lines falling over these channels was measured. Quite often such test lines were divided into two or more parts by cellular projections; in such cases the length of a test line was calculated as the sum of these parts. An example of this is shown: the length of the test line here is $a+b$. The different levels of the epithelium (I–V) are also represented in this figure

The same square lattice – now inclined at an angle of about 20° with the apical plasma membrane (Sitte, 1967; *see also* Fig. 3) – was also used to determine the surface densities of the apical and lateral plasma membranes (S_{Vam} and S_{Vlm}). The paracellular channels were divided into upper and lower halves, where V_{Vpc} and S_{Vlm} were calculated separately. Sitte's method for eliminating the effects of membrane orientation on intersection counts requires that the membranes measured are parallel to each other, or at right angles. By orienting the square lattice with respect to the apical plasma membrane, a bias will remain affecting the measurements of the lateral plasma membranes, since these two sets of membranes are not necessarily perpendicular to each other. The resulting error, however, is probably quite small, since intersections were counted for both sets of lines of the square lattice.

By duplicate measurements in one animal, the error of the method was calculated (*see*, Eränkö, 1955, p. 23). Expressed in per cent of mean values the error for mitochondrial volume density was 11.3%, for nuclear volume density, 5.0%, and for paracellular channel volume density, 3.7%. Calculations of surface densities for the apical and lateral plasma membranes suffered from methodological errors of 5.5% and 3.6%, respectively.

The width of the paracellular channels was also assessed. The arithmetic mean width ($\bar{D}$) was calculated using a formula by Weibel (1973) for estimating the thickness of tissue sheets:

$$\bar{D} = \tfrac{1}{2} \times \bar{L}_3$$

where $\bar{L}_3$ is the mean length of linear intercepts randomly placed over the paracellular channel (*see* Fig. 3 for details). For these measurements the square lattice was placed at random over the channels; the 20° orientation with respect to the apical plasma membrane was thus not adhered to. It is evident from the electron micrographs that the width of the paracellular channels varies considerably in the transporting epithelia. Constrictions are frequently seen (Fig. 2); they do not necessarily surround the entire cell, but might still increase the resistance to fluid transport in the paracellular channel. On p. 46 we discussed how stereological analysis is required to deduce the correct dimensions of a three-dimensional structure from two-dimensional sections, even if the three-dimensional structures are perfectly uniform. In practice, cellular structures are not perfectly uniform but vary in their measurements. How should one average the measured values? It is important to realize that the appropriate method of averaging depends upon the mathematical form in which the structure being measured enters physiological equations. For example, suppose one had a set of pipes of various cross sections. Bulk flow through pipes varies as the fourth power of the radius. Hence if one measured the radii of various pipes and simply calculated an average radius, one would underestimate the actual bulk flow, since small pipes will have been erroneously given equal weight to large pipes. Instead, the effective average radius must be obtained by raising each individual determination to the fourth power, averaging, and then taking the fourth root. On the other hand, if the physiological property of pipes being studied is not bulk flow but is diffusion, then diffusion is proportional to the square of the pipe radius. In this case, individual radius measurements must be weighted as the square power to obtain the correct, effective, average radius. In the present situation, we wish to determine the effective power of radius of cellular channels for evaluating fluid transport. The correct weighting power to be used in averaging will depend upon the particular theory of transport. For example, in the equation for standing gradients (Diamond & Bossert, 1967) there are terms for radius to the first and second power. We shall, therefore, present our results in three different ways: the unweighted arithmetic mean width; the arithmetic mean of widths squared; and the so-called harmonic mean width, which weights width as the inverse power. Naturally, the harmonic widths are all smaller than the arithmetic mean widths (*see* Table 2).

Before the mean width measurements were carried out the channels were divided in five equally wide levels, with the first level (*I*) closest and parallel to the epithelial surface and the fifth level (*V*) closest to the base of the cells (*see* Fig. 3). In this way the channel width could be analyzed at different levels of the paracellular channels. The means are generally based on 60 measurements in each paracellular channel (12 for each level). In each rabbit five channels were measured in the crest epithelium and five in the crypt epithelium.

The height of the transporting epithelium was measured light microscopically. Only such tissue sections where it was possible to follow the individual cells from the base to the lumen were measured.

The increment of the lumen surface area (IC_{LM}) due to folds and crypts was also measured by light microscopy. A straight reference line was drawn roughly parallel to the surface of the epithelium. The square lattice was placed over the picture with the squares tilted to about 20° angle with the straight line (Sitte, 1967). The number of intersections ($=m$) between the lines of the lattice and the surface of the epithelium was counted. Similarly the intersections ($=n$) were counted between the lattice lines and the straight line. The increment of surface area $IC_{LM}=m/n$. The surface enlargement (IC_{EM}) due to microvilli, etc., which require electron microscopy to be seen, was assessed similarly.

On the lateral cell surface cytoplasmic leaflets, interdigitations and microvilli cause an enlargement of the plasma membrane area. Here also the above procedure by electron microscopy was used to find the enlargement factor (IC_{LA}). The straight reference line was drawn roughly perpendicular to the surface of the mucosa. These measurements were performed in five different levels (*I–V*) of the paracellular channels as described above.

Results

Transporting Epithelium

The qualitative morphological information obtained by light and electron microscopy is in good agreement with previous reports on the rabbit gallbladder (Kaye, Wheeler, Whitlock & Lane, 1966; Smulders, Tormey & Wright, 1972; Tormey & Diamond, 1967) Our electron micrographs showed a fairly uniform picture of the transporting gallbladder epithelium. The cells in the crest (Fig. 2) averaged 28 μm in height, and were separated by wide, irregularly formed intercellular spaces. In crypt epithelium (Fig. 4) the cell height averaged 18 μm and the intercellular spaces appeared smaller. The epithelial cells were tall, columnar with the apical cell surface studded with microvilli. Because of such microvilli the area of the apical cell surface on the crests was enlarged by an average factor (IC_{EM}) of 4.6× and in the crypts by a factor of 6.4× (*see also* Table 1). Folds and crypts were responsible for another enlargement of the surface area in comparison with the macroscopic area: this enlargement (IC_{LM}) was calculated to 2.7× (SD 0.58, n=7 animals) (Smulders, Tormey & Wright, 1972, who worked on stretched, mounted gall bladders reported IC_{LD} to be 1.5–1.7×). The total area of the epithelium was thus on

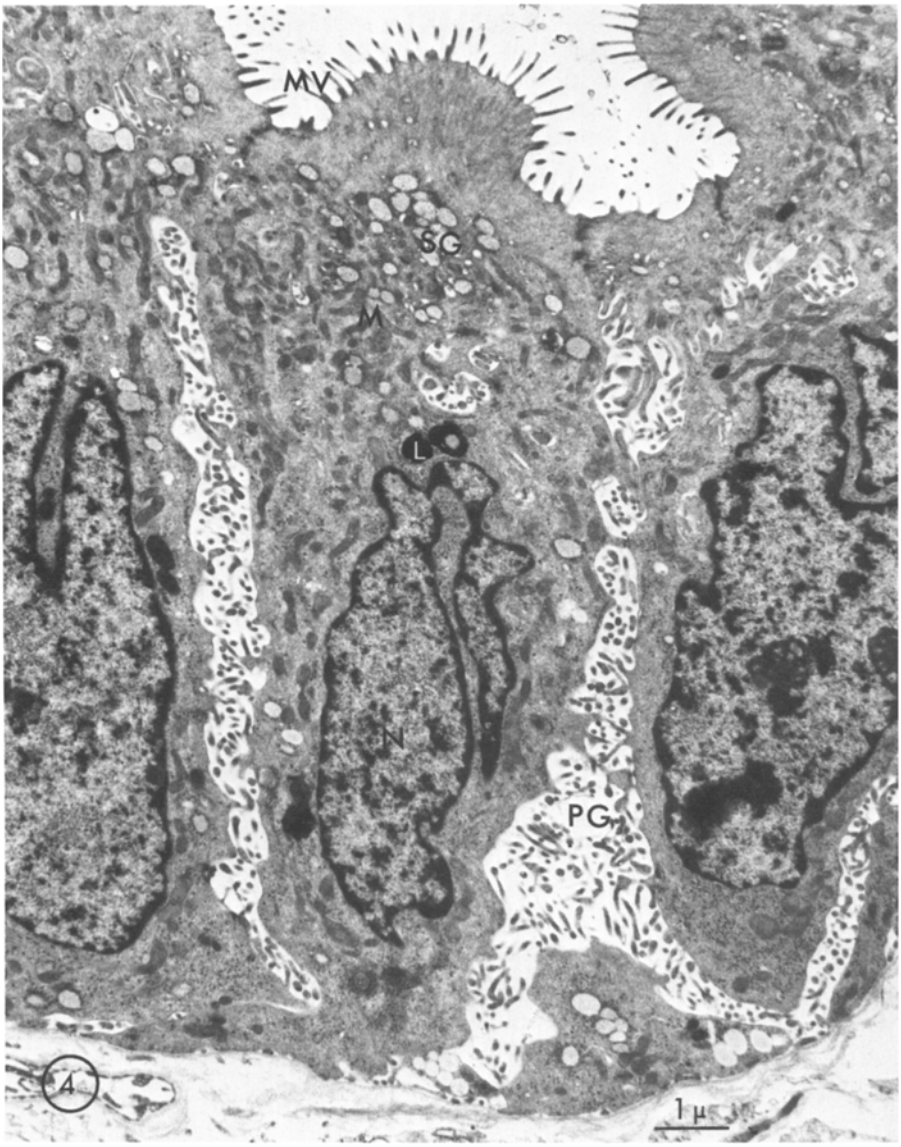

Fig. 4. Survey of in vitro transporting crypt cells. The paracellular channels (*PC*) are narrower than in the crest epithelium. *N*: nucleus; *M*: mitochondria; *MV*: microvilli; *L*: lysosome-like body; *SG*: secretory granules. 8800×

an average $IC_{EM} \times IC_{LM} = 0.5 \times (4.6 + 6.4) \times 2.7 = 14.9$ times the macroscopic area.

The lateral cell surfaces of neighboring cells were closely apposed forming typical occluding zonules close to the apical cell surface. Adhering zonules were observed mainly in level *I* (*cf.* Fig. 3), and beneath these

Table 1. Stereological data from in vitro transporting and ouabain-inhibited gallbladder epithelia (Means ± SD; n = 7 for transporting epithelia, n = 5 for inhibited epithelia)[e]

Structure	Units	State of function	Level in epithelium[a]	Crest epithelium	Crypt epithelium
Nucleus (V_{Vn})	% of cell volume	Transporting	–	16.9 ± 5.0	18.7 ± 4.3
		Inhibited		10.9 ± 4.9	13.4 ± 1.2[c]
Mitochondria (V_{Vmi})	% of cytoplasmic volume	Transporting	–	18.7 ± 5.5	14.1 ± 2.5[b]
		Inhibited		5.9 ± 2.0[c]	4.3 ± 0.6[c]
Paracellular channel (V_{Vpc})	% of epithelial volume	Transporting	–	28.3 ± 6.5	11.0 ± 3.4[b]
			Upper half	20.5 ± 7.3	7.6 ± 3.0[b]
			Lower half	36.1 ± 7.0[d]	14.4 ± 4.6[b,d]
Apical plasma membrane (S_{Vam})	$\mu m^2/\mu m^3$ of cell volume	Transporting	–	0.51 ± 0.09	0.61 ± 0.15[b]
		Inhibited		0.18 ± 0.06[c]	0.26 ± 0.14[c]
Lateral plasma membrane (S_{Vlm})	$\mu m^2/\mu m^3$ of cell volume	Transporting	–	4.09 ± 1.25	2.85 ± 0.95
			Upper half	2.58 ± 0.56	2.35 ± 0.86
			Lower half	5.60 ± 2.11[d]	3.36 ± 1.24[d]
Epithelial height	μm	Transporting	–	28.1 ± 1.7	17.9 ± 1.1[b]
Enlargement factor for apical plasma membrane (IC_{EM})	–	Transporting	–	4.6 ± 0.5	6.4 ± 1.4[b]

[a] When no level is indicated, the data refer to whole epithelium. In the remaining cases the epithelium was divided into upper and lower halves (*see* p. 50).
[b] Significantly different from the corresponding value in crest epithelium ($p < 0.05$).
[c] Significantly different from the corresponding value in transporting epithelium ($p < 0.05$).
[d] Significantly different from the corresponding value in upper half of epithelium ($p < 0.05$).
[e] Student's *t*-test with paired data used when comparing parameters within the transporting epithelia. Nonpaired data were used when comparing transporting and inhibited epithelia.

cell contacts there were extensive paracellular channels with numerous fingerlike evaginations or leaflets projecting from the lateral cell surfaces. In relation to the epithelial volume, the paracellular channels were $2\frac{1}{2}$ times larger in the crest epithelium than in the crypt epithelium (28 *vs.* 11%) (Table 1). Both in the crest and in the crypt epithelium these channels were roughly twice as large in the basal half of the epithelium as in the apical half.

We also calculated how many times larger the lateral plasma membrane area is than the area of smooth straight cylinders of similar size

Table 2. Dimensions at different epithelial levels for paracellular channel, and enlargement factors for the lateral plasma membrane in transporting gallbladder epithelia (Means ± SD; n = 7)

	Location	Level I	Level II	Level III	Level IV	Level V	All levels combined
Arithmetic mean width (μm)	Crest	0.39 ±0.47	1.09 ±0.74	1.26 ±0.78	1.14 ±0.74	0.78 ±0.49	0.93 ±0.62
	Crypt	0.12 ±0.04	0.21 ±0.09	0.27 ±0.15	0.30 ±0.13	0.27 ±0.12	0.24 ±0.10[a]
Harmonic mean width (μm)	Crest	0.19 ±0.25	0.85 ±0.74	1.07 ±0.72	0.94 ±0.70	0.51 ±0.27	0.38 ±0.37
	Crypt	0.075 ±0.02	0.159 ±0.072	0.230 ±0.160	0.255 ±0.126	0.206 ±0.113	0.134 ±0.052[a]
Arithmetic mean of widths squared (μm^2)	Crest	0.532 ±1.121	2.260 ±3.062	2.942 ±3.493	2.436 ±2.900	1.158 ±1.608	1.843 ±2.409
	Crypt	0.023 ±0.033	0.068 ±0.093	0.127 ±0.126	0.148 ±0.122	0.124 ±0.096	0.098 ±0.078[a]
Enlargement factor for lateral plasma membrane (IC_{LA})	Crest	4.4 ±0.8	3.9 ±0.6	3.1 ±0.4	3.0 ±0.4	3.2 ±0.5	3.5 ±0.3
	Crypt	3.0 ±0.6	3.4 ±0.6	3.1 ±0.4	3.4 ±0.5	3.1 ±0.4	3.2 ±0.4
"Effective diameter" (μm)	Crest	–	–	–	–	–	0.29 ±0.18
	Crypt	–	–	–	–	–	0.16 ±0.05[a]

[a] Significantly lower value than in crest epithelium ($p < 0.05$; Student's t-test was used with pairing of data). Tests of significance were carried out only in the last column.

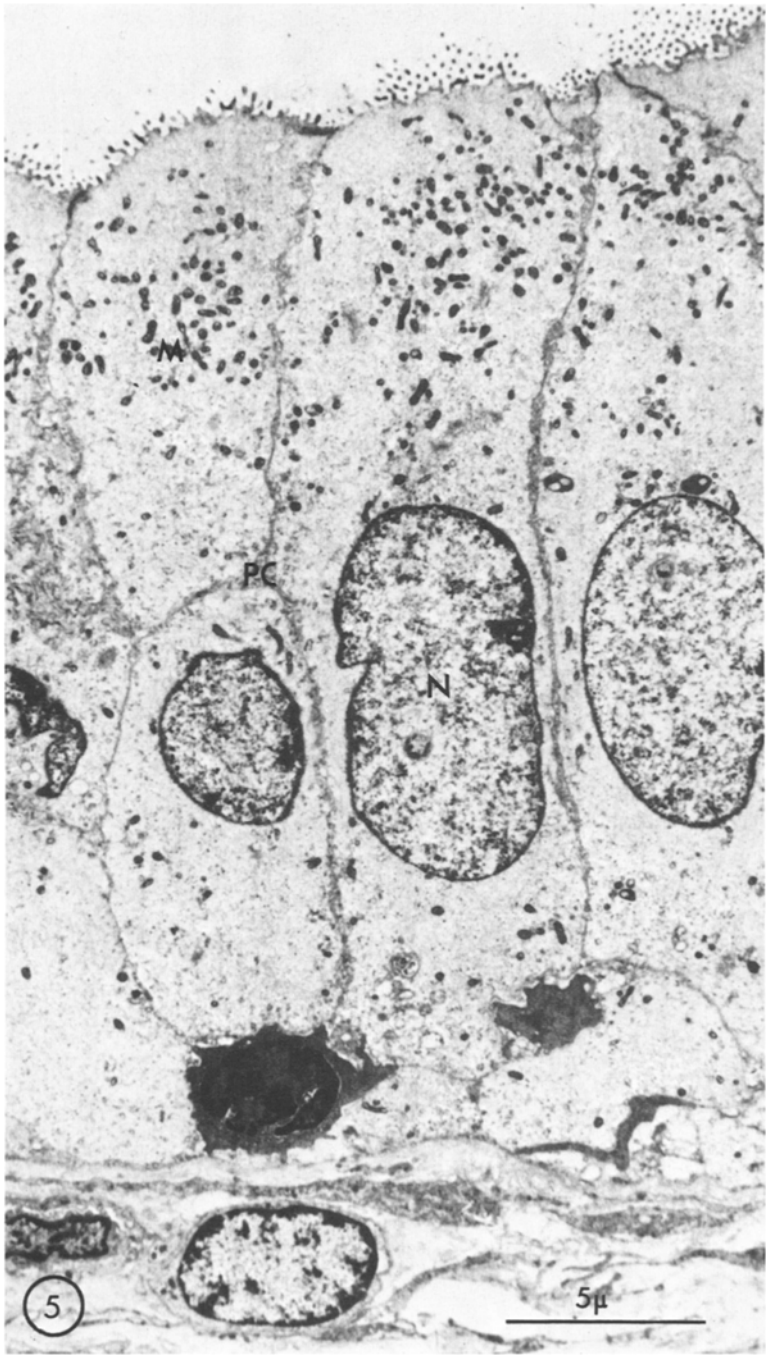

Fig. 5. Survey of ouabain-inhibited crypt cells. The paracellular channels (*PC*) appear collapsed and the cells are swollen. *N*: nucleus; *M*: mitochondria. 5300×

as the epithelial cells. Figures on the enlargement factors (IC_{LA}) for each level can be found in Table 2; they varied between 3 and 4.4×.

The arithmetic mean width of the intercellular channels was almost 4 times larger in the crest epithelium than in the crypt epithelium (0.93 *vs.* 0.24 μm). Data on harmonic mean widths and squared widths can be found in Table 2.

The cell nuclei were found at about midheight of the cells and occupied roughly 1/6 of the cell volume. About 16% of the cytoplasm was taken up by mitochondria: most of these were found in the supranuclear part.

Ouabain Inhibited Epithelium

The main difference between the transporting and the ouabain inhibited epithelia related to the paracellular channels. After ouabain treatment these channels had uniformly shrunk to about 20 nm in width, and the mitochondria occupied a significantly smaller relative volume of the cytoplasm (Fig. 5, Table 1); the latter reflected a substantial swelling of the cells. By light microscopy the cell height on the crests averaged 80 nm, but since it was difficult to judge whether the epithelium was sectioned perpendicular to the surface, this figure suffers from certain errors.

Discussion

In their classical article on standing gradient osmotic flow across epithelia Diamond and Bossert (1967) discussed factors which might influence the osmolarity of the fluid emerging from the basal end of the paracellular channels. In order to obtain a simple representation of the flow system, they used a right circular cylindrical channel closed at one end and open at the other as a model for the paracellular channel. In this model the osmolarity of the fluid emerging from the open end of the channel (at the base of the epithelium) was given by the expression:

$$O_s = \frac{2\pi r \int_{x=0}^{x=L} N(x)dx}{\pi r^2 v(L)}$$

where r is the radius of the channel, x the position in the channel (at the closed end $x=0$, and at open end $x=L$), $N(x)$ is the rate of active solute transport across the walls of the channel into the lumen

at any height x (mosmoles per sec per cm^2 of channel wall area), and $v(L)$ the velocity of fluid flow in the channel at the open end of the channel.

The height of the gallbladder epithelium was 28 and 18 μm for crest and crypt epithelium, respectively. Tormey and Diamond (1967) gave the slightly higher figure of 32 μm for the height of the paracellular channels. Because of cellular interdigitations the paracellular channels are obviously much longer. In a few electron micrographs we traced the shortest way through the paracellular channels, from the *zonula occludens* to the basement membrane. This distance was 1.5–4 times longer than the straight distance. It may thus be assumed that the length of the paracellular channels usually lies between 40 and 120 μm, well within the limits of the 4–200 μm suggested by Diamond and Bossert (1967).

Tormey and Diamond (1967) also measured the channel width by light microscopy of OsO_4 fixed Epon sections; these measurements were performed at a level halfway between the luminal and basal surfaces of the epithelium. In transporting epithelia they obtained an average intercellular channel width of 0.88 μm (1.52 μm for crest epithelium and 0.57 μm for crypt epithelium), which is larger than our arithmetic mean widths for level III of 1.26 μm and 0.27 μm, respectively. Our values are surely more nearly correct than those of Tormey and Diamond, because these investigators used the light microscope, in which many of the interdigitating cell processes are below the limit of resolution (less than 0.2 μm) and the channel widths were therefore overestimated.

It should be emphasized that although our width values are based on a large number of measurements (more than 4000), several types of errors may occur. In using Weibel's (1973) formula (*see* p. 50) we implied that the paracellular channels were tissue sheets of random orientation. Since we tried to section perpendicular to the surface of the mucosa (*see* p. 47), the paracellular channels were, strictly speaking, not randomly oriented during the subsequent measuring. However, due to the tortuosity of the channels the bias thus introduced should be of minor importance and acceptable for the purpose of the present study. Sectioning completely at random would have ruined the possibilities of distinguishing between crest and crypt epithelium.

Another factor of unknown significance is the glycoprotein coating on the lateral cell surface. This coating, which is not visualized in our electron micrographs, will reduce the width of the paracellular channels (*see also* Smulders, Tormey & Wright, 1972). A third source of error is the swelling and/or shrinkage of the tissue components during the processing of the tissue (further discussed on pp. 58–60).

The paracellular channels are obviously no right circular cylinders, but rather a system of interconnected tissue sheets of highly varying thickness. Because of the irregular architecture, Hill (1975) (*see also* Segel, 1970) recommended the use of the "effective radius" of the paracellular channels, which equals $2a/c$, representing twice the area divided by the circumference. On the basis of our stereological data we have calculated the "effective diameter" to 290 nm in the crests and 160 nm in the crypts.

Segel (1970) derived an analytical approximation in which the ratio of the emergent osmolarity O_s to the osmolarity of the bathing fluid C_o could be calculated. In these equations the morphometric expression L^2/r played an important role. This expression was also discussed by Hill (1975), who suggested that L^2/r must exceed 50 cm if the emergent fluid should be near isotonic. Hill's figure was based on the assumption that the osmotic water permeability (L_p) was 10^{-5} cm sec^{-1} $osmol^{-1}$, but higher L_p values—up to 8×10^{-3} or more—have recently been suggested (Diamond, 1977). With higher L_p the required L^2/r values decreases. In his article Hill presented data from 13 publications showing that L^2/r did not exceed 1 cm in any of the 11 epithelia investigated. This evidence was used by Hill to reject the standing gradient model. However, it must be emphasized that *in none of these articles were stereological methods employed,* and for that reason their data must be handled with great care. In the present study, using an estimate of 80 μm for the paracellular channel length in transporting crest epithelium we obtain values for L^2/r of 1.4, 3.4 or 4.4 cm, respectively, depending on whether the arithmetic mean "radius" (465 nm), the harmonic mean "radius" (190 nm), or the "effective radius" (145 nm) is used in the denominator. Our stereological data thus seem compatible with the standing gradient model.

A major concern in stereological studies is the morphological alterations which are brought about by fixation (*see* Smulders, Tormey & Wright, 1972), dehydration, and embedding of the tissue. Frederiksen and Rostgaard (1974) reported the absence of dilated lateral intercellular spaces in the frog gallbladder epithelium. By Nomarski interference light microscopy they could not observe such spaces in the living in vitro transporting epithelium. Although not stated by the authors, the optical resolution in their 400–500 μm thick system can be estimated to 1–2 μm. During dehydration and embedding in Epon there appeared to be a shrinkage of the cells, and intercellular spaces appeared. These observations deserve considerable attention. The authors also reported

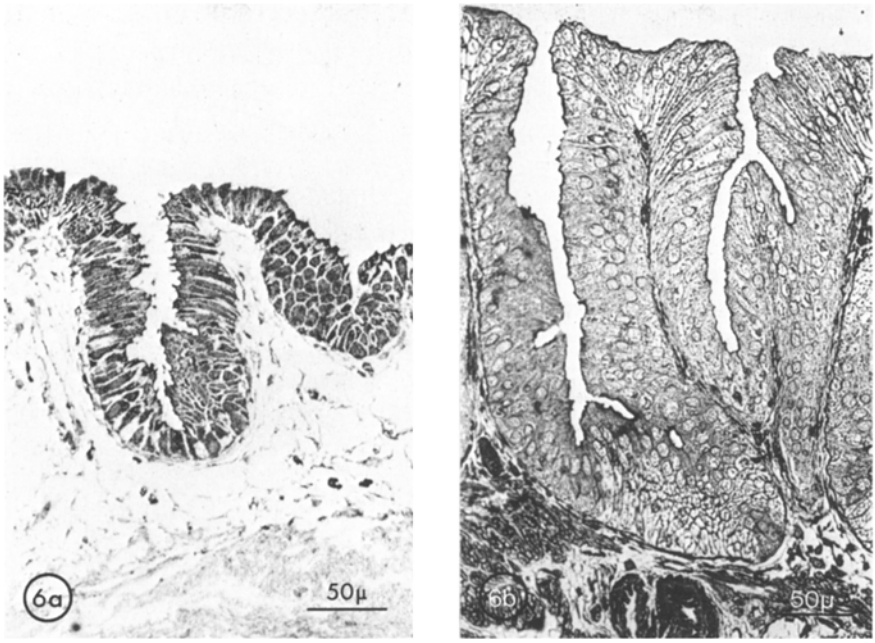

Fig. 6. Light micrographs of in vitro transporting (*6a*) and ouabain inhibited (*6b*) epithelia. The specimens were frozen in liquid isopentan (−150 °C) and dried at −45 °C. After embedding in Epon; 1-µm thick sections were cut and contrasted with toluidine blue. Paracellular channels are readily observed in the transporting epithelium, but are not seen in the inhibited epithelium. 210×

preliminary results from ouabain inhibited frog gallbladder, in which they did not observe any dilated lateral intercellular spaces, neither in the living state, nor during or after the processing of the tissue, and suggested that the interference by ouabain with cell membrane permeability, ion pumps, and/or contractile mechanisms should prevent the shrinkage of these cells during processing. This is difficult to reconcile with the findings that OsO_4, which was used in this case, brings about a denaturation of the tissue, leading to a very high permeability for osmotically active substances (Smulders, Tormey & Wright, 1972; Helander, Rehm & Sanders, 1973). This opening up of channels into the cells should be no less effective in the transporting gallbladder than in the inhibited one. Moreover, large differences exist between the in vitro gallbladders from frogs and from rabbits. The transport rate in the frog gallbladders was only 11 mg per hr per cm^2, whereas Tormey and Diamond (1967) reported a rate of 388 µl per gallbladder and per hr, corresponding to 86 mg per hr per cm^2 (the gallbladders in our experi-

ments measured about 4.5 cm^2). With a transport rate of less than 15% in the frog as compared to the rabbit, one would thus expect much smaller paracellular channels than in the rabbit gallbladder, provided that the cell size is similar.

In order to elucidate this problem further we fixed a few transporting and a few ouabain inhibited rabbit gallbladders by freezing in liquid isopentan (at about −150 °C) and then dried the specimens at −45 °C in a freeze-drier equipped with an oil diffusion pump. After a few days the tissue was dry, judging from the pressures recorded when increasing the temperature. Dry OsO_4 vapor was let into the chamber to react with the tissue for about 16 hr. The specimens were then infiltrated for 6 hr in Epon, and polymerized at 37° for 24 hr and at 60° for 24 hr. One-micron sections were cut from the embedded tissues, stained with toluidine blue and studied in the light microscope.

Light micrographs of freeze-dried tissues are shown in Fig. 6. Dilated lateral intercellular spaces were clearly seen in the transporting gallbladder epithelium, but were absent from the ouabain-inhibited ones. In this aspect no differences were found against tissues fixed with formalin, such as can be seen in Fig. 1. In our opinion this constitutes a strong indication of the presence of such spaces in the living, in vitro transporting rabbit gallbladder epithelium.

This work was supported by grants from the Swedish Medical Research Council (project no. 12X-2298) and from the Medical Faculty of the University of Umeå.

References

Diamond, J.M. 1977. The epithelial junction: Bridge, gate and fence. *Physiologist (in press)*

Diamond, J.M., Bossert, W.H. 1967. Standing-gradient osmotic flow. A mechanism for coupling water and solute transport in epithelia. *J. Gen. Physiol.* **50**:2061

Eränkö, O. 1955. Quantitative Methods in Histology and Microscopic Histochemistry. Karger, Basel

Frederiksen, O., Rostgaard, J. 1974. Absence of dilated lateral intercellular spaces in fluid-transporting frog gallbladder epithelium. *J. Cell Biol.* **61**: 830

Helander, H.F., Rehm, W.S., Sanders, S.S. 1973. Influence of fixation on physiological properties of frog gastric mucosa. *Acta Physiol. Scand.* **88**:109

Hill, A.E. 1975. Solute-solvent coupling in epithelia: A critical examination of the standing-gradient osmotic flow theory. *Proc. R. Soc. London B.* **190**:99

Kaye, G.I., Wheeler, H.O., Whitlock, R.T., Lane, N. 1966. Fluid transport in the rabbit gall bladder. A combined physiological and electron microscopic study. *J. Cell Biol.* **30**:237

Segel, L.A. 1970. Standing-gradient flows driven by active solute transport. *J. Theor. Biol.* **29**:233

Sitte, H. 1967. Morphometrische Untersuchungen an Zellen. *In:* Quantitative Methods in Morphology. E.R. Weibel and H. Elias, editors. p. 167. Springer-Verlag, Berlin

Smulders, A.P., Tormey, J.McD., Wright, E.M. 1972. The effect of osmotically induced water flows on the permeability and ultrastructure of the rabbit gallbladder. *J. Membrane Biol.* **7**:164

Tormey, J.McD., Diamond, J.M. 1967. The ultrastructural route of fluid transport in rabbit gall bladder. *J. Gen. Physiol.* **50**:2031

Weibel, E.R. 1969. Stereological principles for morphometry in electron microscopic cytology. *Int. Rev. Cytol.* **26**:235

Weibel, E.R., Bolender, R.P. 1973. Stereological techniques for electron microscopic morphometry. *In:* Principles and Techniques of Electron Microscopy. M.A. Hayat, editor. Vol. 3, pp. 237–269. van Nostrand Reinhold, New York

Wright, E.M., Smulders, A.P., Tormey, J.McD. 1972. The role of the lateral intercellular spaces and solute polarization effects in the passive flow of water across the rabbit gallbladder. *J. Membrane Biol.* **7**:198